

# Compressed sensing with sparse, structured matrices

Maria Chiara Angelini

Dip. Fisica

Università La Sapienza

P.le Aldo Moro 5, 00185 Roma, Italy

Email: Maria.Chiara.Angelini@roma1.infn.it

Federico Ricci-Tersenghi

Dip. Fisica, CNR – IPCF, UOS Roma

INFN – Roma 1, Università La Sapienza

P.le Aldo Moro 5, 00185 Roma, Italy

Email: Federico.Ricci@roma1.infn.it

Yoshiyuki Kabashima

Dept. of Comput. Intell. & Syst. Sci.

Tokyo Institute of Technology

Yokohama 226-8502, Japan

Email: kaba@dis.titech.ac.jp

**Abstract**—In the context of the compressed sensing problem we propose a new ensemble of sparse random matrices which allow (i) to acquire/compress a  $\rho_0$ -sparse signal of length  $N$  in a time linear in  $N$  and (ii) to perfectly recover the original signal, compressed at a rate  $\alpha$ , by using a message passing algorithm (Expectation Maximization Belief Propagation) that runs in a time linear in  $N$ . In the large  $N$  limit, the scheme proposed here closely approach the theoretical bound  $\rho_0 = \alpha$ , and so it is both optimal and efficient (linear time complexity). More generally, we show that several ensembles of dense random matrices can be converted into ensembles of sparse random matrices, having the same thresholds, but much lower computational complexity.

## I. INTRODUCTION

Compressed sensing is a framework that enables to recover an  $N$ -dimensional sparse signal  $\mathbf{s} = (s_i)$  from  $M (< N)$  linear measurements of its elements,  $\mathbf{y} = \mathbf{F}\mathbf{s}$ , exploiting the prior knowledge that  $\mathbf{s}$  contains many zero elements [1]. A simple consideration guarantees that the  $\ell_0$ -recovery

$$\hat{\mathbf{s}} = \underset{\mathbf{x}}{\operatorname{argmin}} \|\mathbf{x}\|_0 \quad \text{subj. to} \quad \mathbf{y} = \mathbf{F}\mathbf{x}, \quad (1)$$

where  $\|\mathbf{x}\|_0$  denotes the number of non-zero elements in  $\mathbf{x}$ , is theoretically optimal in terms of minimizing the number of measurements  $M$  necessary for perfectly recovering any original signal  $\mathbf{s}$ . However, carrying out the  $\ell_0$ -recovery for a general measurement matrix  $\mathbf{F}$  is NP-hard. For avoiding such computational difficulty, an alternative approach, the  $\ell_1$ -recovery

$$\hat{\mathbf{s}} = \underset{\mathbf{x}}{\operatorname{argmin}} \|\mathbf{x}\|_1 \quad \text{subj. to} \quad \mathbf{y} = \mathbf{F}\mathbf{x}, \quad (2)$$

where  $\|\mathbf{x}\|_1 = \sum_{i=1}^N |x_i|$ , is widely employed, as (2) is generally converted to a linear programming problem and therefore signal recovery is mathematically guaranteed in an  $O(N^3)$  computational time by use of the interior point method. Nevertheless, the  $O(N^3)$  cost of computation can still be unacceptable in many practical situations, and much effort is being made for exploring more computationally feasible and accurate recovery schemes [2]–[7].

Among such efforts, a recovery scheme recently proposed by Krzakala et al. [7] is worth of attention. Their scheme basically follows the Bayesian approach. Namely, the signal recovery problem is formulated as that of statistical inference from the posterior distribution

$$P(\mathbf{x}|\mathbf{F}, \mathbf{y}) = \frac{\delta(\mathbf{F}\mathbf{x} - \mathbf{y})P(\mathbf{x})}{Z(\mathbf{F}, \mathbf{y})}, \quad (3)$$

where  $Z(\mathbf{F}, \mathbf{y})$  is a normalization factor imposing the condition  $\int d\mathbf{x} P(\mathbf{x}|\mathbf{F}, \mathbf{y}) = 1$  and a component-wise prior distribution  $P(\mathbf{x}) = \prod_{i=1}^N [(1 - \rho)\delta(x_i) + \rho\phi(x_i)]$  is assumed.  $\rho$  and  $\phi(x)$  represent the density of non-zero signal elements and a Gaussian distribution, respectively. Exactly inferring  $\mathbf{s}$  from (3) is NP-hard similarly to (1). However, by employing the belief propagation (BP) in conjunction with the expectation-maximization (EM) algorithm for estimating  $\rho$  and the parameters of  $\phi(x)$ , they developed an approximation algorithm, termed EM-BP, which overcomes the recovery performance of (2) with an only  $O(N^2)$  computational cost. Furthermore, they showed that, by employing a peculiar type of “seeded” matrix  $\mathbf{F}$ , the threshold value of the compression rate  $\alpha = M/N$  of EM-BP, above which the original signal is typically recovered successfully, can approach very close to that of the  $\ell_0$ -recovery,  $\alpha_{s-EMBP} = \rho_0$ , where  $\rho_0$  is the actual signal density of  $\mathbf{s}$  and  $s-EMBP$  stands for ‘seeded EM-BP’. The seeded matrix is composed of blocks along the diagonal densely filled with Gaussian random variables. It is important to remember that this result is achieved for the first time with an approach different from the  $\ell_0$ -recovery, being the threshold for the  $\ell_1$ -recovery much higher than the optimal one:  $\alpha_{\ell_1} > \rho_0$ . As the optimality of the  $\ell_0$ -recovery is guaranteed for the EM-BP, this indicates that this scheme can practically achieve the theoretically optimal threshold of the signal recovery with an  $O(N^2)$  computational cost. However, the optimality of their scheme in terms of the computational complexity is still unclear; there might be a certain design of the measurement matrix  $\mathbf{F}$  that makes it possible to further reduce the necessary computational cost keeping the same signal recovery threshold.

The purpose of the present work is to explore such a possibility. For this, we focus on a class of matrices that are characterized by the following properties:

- **sparsity:** The matrix  $\mathbf{F}$  has only  $O(1)$  non-zero elements per row and column. This implies that the measurements can be performed in a time linear in the signal length. This is highly preferred for practicality, given that such an operation typically needs to be done in real time, during data acquisition.
- **integer values:** The matrix elements are not real valued, but take small integer values. This means that an optimized code for the measurements can work with bitwise

operations, thus achieving much better performance without any loss of precision.

- **no block structure:** The block structure used in [7] may not be necessary for reaching the optimal threshold. As an alternative possibility, we study a structure made of a square matrix in the upper left corner (the seed) plus a stripe along the diagonal. This structure is much more amenable for analytic computations, since it corresponds to a one-dimensional model homogeneous in space.

The use of sparse matrices for compressed sensing has already been proposed in several earlier studies [8]–[12]. Among them, our approach is particularly similar to that of [12] in the sense that the both sides are based on the Bayesian framework and use integer-valued sparse measurement matrices. Nevertheless, the two approaches differ considerably in the following two points. Firstly, we adopt EM-BP, which updates only a few variables per node for the signal recovery, while the recovery algorithm of [12] involves functional updates and needs significantly more computational time than ours. Secondly, we make much effort to explore a simple design of  $\mathbf{F}$  that achieves a nearly optimal recovery performance while the problem of the matrix design is not fully argued in [12]. By carrying out extensive numerical experiments in conjunction with an analysis based on density evolution [13], we show that a threshold close to the theoretical limit  $\alpha = \rho_0$  can be achieved by the matrices with the above properties with almost *linear* computational cost in both measurement and recovery stages.

This paper is organized as follows. In Section II the EM-BP algorithm is briefly explained and the results for dense matrices are summarized. The algorithm is applied to homogeneously sparse matrices in Section III and to structured sparse block matrices in Section IV. A new type of “striped” sparse matrix without blocks is introduced in Section V. The last Section summarizes the work focusing on its importance for practical use and on perspectives.

## II. EXPECTATION MAXIMIZATION BELIEF PROPAGATION

The new algorithm based on BP in conjunction with EM proposed in Ref. [7] starts from Eq. (3). In order to solve it with BP,  $O(MN)$  messages for the probability distributions of the variables  $x_i$  are constructed in the following way:

$$m_{\mu \rightarrow i}(x_i) = \frac{1}{Z^{\mu \rightarrow i}} \int \prod_{j \neq i} dx_j m_{j \rightarrow \mu}(x_j) \delta\left(y_\mu - \sum_k F_{\mu k} x_k\right)$$

$$m_{i \rightarrow \mu}(x_i) = \frac{1}{Z^{i \rightarrow \mu}} \left[ (1 - \rho) \delta(x_i) + \rho \phi(x_i) \right] \prod_{\gamma \neq \mu} m_{\gamma \rightarrow i}(x_i)$$

where  $Z^{i \rightarrow \mu}$  and  $Z^{\mu \rightarrow i}$  are normalization factors. This EM-BP equations are very complicated because the messages are distribution functions. In order to make them simpler, the messages can be approximated assuming that they are Gaussian, thus obtaining the equations for the mean  $a_{i \rightarrow \mu}$  and the variance  $v_{i \rightarrow \mu}$  of  $m_{i \rightarrow \mu}(x_i)$ . This approximation was firstly introduced for sparse matrices in Ref. [14] and it becomes exact asymptotically if  $\mathbf{F}$  is dense. In fact it

derives from an expansion in small  $F_{\mu i}$ , and in the dense case  $F_{\mu i} = O(1/\sqrt{N})$ . Supposing that the elements of the original signal follow a Bernoulli-Gaussian distribution with parameters  $\rho_0$ ,  $\bar{x}_0$  and  $\sigma_0$ , the update rules for the messages are the following:

$$a_{i \rightarrow \mu} = f_a \left( \sum_{\gamma \neq \mu} A_{\gamma \rightarrow i}, \sum_{\gamma \neq \mu} B_{\gamma \rightarrow i} \right)$$

$$a_i = f_a \left( \sum_{\gamma} A_{\gamma \rightarrow i}, \sum_{\gamma} B_{\gamma \rightarrow i} \right)$$

$$v_{i \rightarrow \mu} = f_c \left( \sum_{\gamma \neq \mu} A_{\gamma \rightarrow i}, \sum_{\gamma \neq \mu} B_{\gamma \rightarrow i} \right)$$

$$v_i = f_c \left( \sum_{\gamma} A_{\gamma \rightarrow i}, \sum_{\gamma} B_{\gamma \rightarrow i} \right)$$

$$A_{\mu \rightarrow i} = \frac{F_{\mu i}^2}{\sum_{j \neq i} F_{\mu j}^2 v_{j \rightarrow \mu}}$$

$$B_{\mu \rightarrow i} = \frac{F_{\mu i} \left( y_\mu - \sum_{j \neq i} F_{\mu j} a_{j \rightarrow \mu} \right)}{\sum_{j \neq i} F_{\mu j}^2 v_{j \rightarrow \mu}} \quad (4)$$

where  $f_a$  and  $f_c$  are some analytical functions depending on the parameters  $\rho$ ,  $\bar{x}$  and  $\sigma$ . For details, see Ref. [7].

In general, the original  $\rho_0$ ,  $\bar{x}_0$  and  $\sigma_0$  are not known, but one can use EM to derive the update rules for them, using the property that the partition function

$$Z(\rho, \bar{x}, \sigma) = \int d\mathbf{x} P(\mathbf{x}) \delta(\mathbf{y} - \mathbf{F}\mathbf{x})$$

is the likelihood of the parameters  $(\rho, \bar{x}, \sigma)$  and is maximized by the true parameters  $\rho_0$ ,  $\bar{x}_0$  and  $\sigma_0$ . Thus, after the update of all the messages, the inferred parameters of the original distribution are updated following these rules:

$$\bar{x} \leftarrow \frac{1}{\rho N} \sum_i a_i, \quad \sigma^2 \leftarrow \frac{1}{\rho N} \sum_i (v_i + a_i^2) - \bar{x}^2,$$

$$\rho \leftarrow \frac{\sum_i \frac{1/\sigma^2 + U_i}{V_i + \bar{x}/\sigma^2} a_i}{\sum_i \left[ 1 - \rho + \frac{\rho}{\sigma(1/\sigma^2 + U_i)^{\frac{1}{2}}} e^{\frac{(V_i + \bar{x}/\sigma^2)^2 - \bar{x}^2}{2\sigma^2}} \right]^{-1}},$$

with  $U_i = \sum_{\gamma} A_{\gamma \rightarrow i}$  and  $V_i = \sum_{\gamma} B_{\gamma \rightarrow i}$ .

If the algorithm converges to the correct solution,  $a_i = s_i$  and  $v_i = 0$ .

To reduce the number of messages from  $O(NM)$  to  $O(N)$ , one can notice that in the large  $N$  limit, the messages  $a_{i \rightarrow \mu}$  and  $v_{i \rightarrow \mu}$  are nearly independent of  $\mu$ . Thus equations involving only a variable per each measurement node and a variable per each signal node can be derived, being careful to keep the correcting Onsager reaction term as for the TAP equations in statistical physics [15]. This method was introduced in the context of compressed sensing in Ref. [6] and is called approximated message passing (AMP).

In general, the correct distribution of the original signal is unknown. However, in Ref. [7] it is demonstrated that if

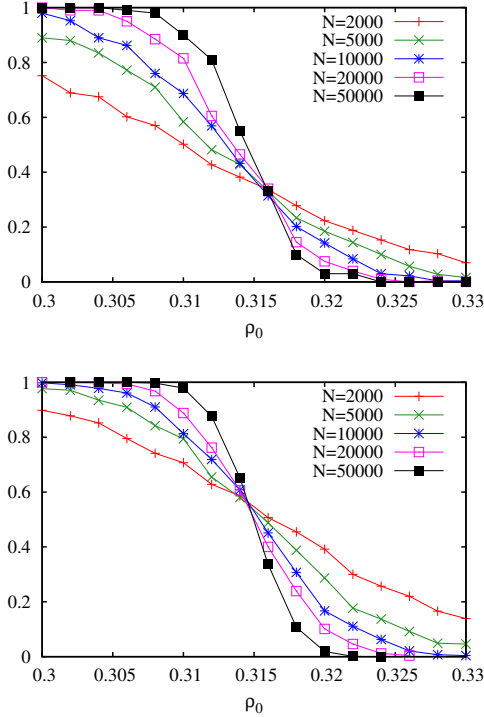


Fig. 1. Top: Probability of perfect recovery versus the signal sparsity  $\rho_0$  using sparse matrices with  $\alpha = 0.5$  and  $K = 20$ . The threshold is the same as with dense matrices. Bottom: Probability of perfect recovery computed with density evolution has the same threshold. Here  $N$  is the population size.

$\alpha > \rho_0$ , the most probable configuration of  $\mathbf{x}$  with respect to  $P(\mathbf{x}) = \prod_{i=1}^N [(1 - \rho)\delta(x_i) + \rho\phi(x_i)]$  with  $\rho < 1$ , restricted to the subspace  $\mathbf{y} = \mathbf{F}\mathbf{x}$ , is the original signal  $\mathbf{s}$ , even if the signal is not distributed according to  $P(\mathbf{x})$ . So our choice of a Gaussian distribution for  $\phi(x)$  should be perfectly fine also even if the original signal has a different distribution.

If a dense matrix is used, the free entropy  $\Phi(D)$  at fixed mean square error  $D = (1/N)\sum_{i=1}^N (x_i - s_i)^2$  can be computed. For  $\alpha > \rho_0$ , the global maximum of the function  $\Phi(D)$  is at  $D = 0$ , that corresponds to the correct solution. However, below a certain threshold  $\alpha < \alpha_{BP}$  that depends on the distribution  $P(s)$ , the free entropy develops a secondary, local maximum at  $D \neq 0$ . As a consequence, the EM-BP algorithm can not converge to the correct solution for  $\rho_0 < \alpha < \alpha_{BP}$ , because a dynamical transition occurs. Nonetheless, the threshold  $\alpha_{BP}$  is lower than  $\alpha_{\ell_1}$ .

### III. EM-BP WITH A SPARSE MATRIX

First of all we want to verify if the use of a sparse matrix can reach the same results than the use of a dense one. For a sparse random matrix the AMP equations can not be used, thus we use the update rules in Eq. (4), for the inference of the original signal  $\mathbf{s}$ . In particular, we choose the matrix  $\mathbf{F}$  to have only  $K = O(1)$  elements different from zero in each row and  $H = \alpha K = O(1)$  elements in each column, extracting them

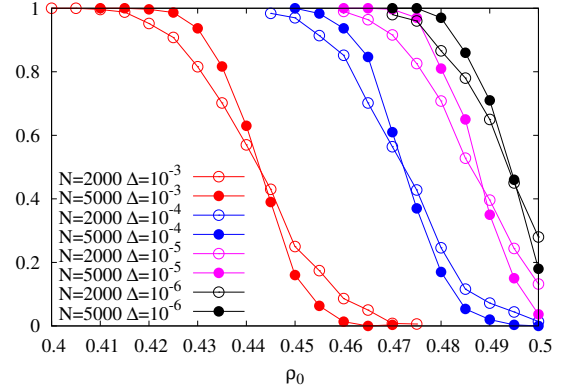


Fig. 2. Stability check for the correct solution under the EM-BP message passing algorithm. Starting the recovery process with a sparse matrix from an initial condition differing less than  $\Delta$  from the correct solution, the latter is recovered as long as  $\rho_0 < \alpha_{stab}(\Delta)$ . In the limit  $\Delta \rightarrow 0$  the stability limit  $\alpha_{stab}(\Delta)$  tends to the theoretical bound  $\alpha$  (which is 0.5).

from the distribution

$$P(F_{\mu i}) = \frac{1}{2}\delta(F_{\mu i} - J) + \frac{1}{2}\delta(F_{\mu i} + J) \quad (5)$$

with  $J = 1$ . The use of the messages  $a_{i \rightarrow \mu}(x)$  and  $v_{i \rightarrow \mu}(x)$  instead of the AMP equations does not involve an extra cost in memory, because, due to the sparsity of the matrix, the number of the messages is  $O(N)$ . In principle the messages  $m_{i \rightarrow \mu}(x)$  are not Gaussian if the matrix is sparse, so the use of only the two parameters  $a_{i \rightarrow \mu}(x)$  and  $v_{i \rightarrow \mu}(x)$  is not exact. However, the convolution of  $K$  messages (with  $K = 20$  in a typical matrix we use) is not far from a Gaussian and indeed we can verify a posteriori that this approximation is valid, because it gives good results.

In all our numerical simulations we use a Bernoulli-Gaussian distributed signal and a compression rate  $\alpha = 0.5$ .

In Fig. 1 (top) the probability of a perfect recovery as a function of the sparsity of the signal  $\rho_0$  for different sizes is shown, applying the EM-BP algorithm using a sparse matrix with  $K = 20$ . The threshold for the perfect recovery in the thermodynamic limit ( $N \rightarrow \infty$ ) is  $\rho_{BP} \simeq 0.315$ , that is the same obtained in Ref. [7] with a dense matrix. We can not analytically compute the free entropy  $\Phi(D)$  as in [7], because we are using sparse matrices and methods such as the saddle point one can not be used. However we can perform a numerical density evolution analysis, as shown in Fig. 1 (bottom) and the threshold is the same as the one computed with the matrices  $\mathbf{F}$ .

Next, we have verified that the correct solution is always the global maximum of  $\Phi(D)$  and it is locally stable up to  $\alpha \simeq \rho_0$  using EM-BP with a sparse matrix. Since we can not compute analytically the free entropy, we must resort to a numerical method. We start EM-BP with an initial condition very close to the correct solution:  $a_{i \rightarrow \mu}^0 = s_i + \delta_{i \rightarrow \mu}$ , with  $\delta_{i \rightarrow \mu}$  a random number uniformly distributed in  $[-\Delta, \Delta]$ . In this way we have verified (see Fig. 2) that if  $\Delta$  is sufficiently

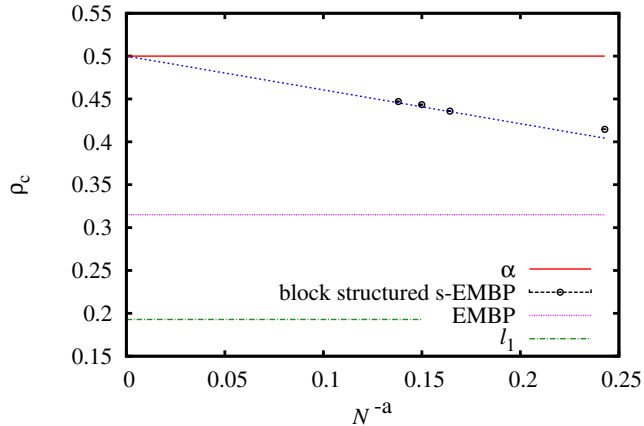


Fig. 3.  $\rho_c(N)$  with a sparse, structured matrix with blocks, for different sizes  $N$  and values of  $L$  (see text). The thresholds for the  $\ell_1$ -recovery and for EM-BP without any structure are also drawn. For comparison with data in Fig. 5, we have used the same exponent  $a \simeq 0.18$  best fitting those data.

small, the correct solution can be found up to  $\alpha \simeq \rho_0$ , as in the case of a dense matrix.

For the algorithms based on the  $\ell_1$  minimization, it is known that the threshold with a sparse matrix is lower than that with a dense one. However, those algorithms are not optimal, because the correct solution disappears below the threshold  $\alpha_{\ell_1}$ . In this sense, the EM-BP algorithm is optimal, because the global maximum of the free entropy is always on the correct solution. Thus one can expect that, if the rank of the sparse matrix is the same as that of the dense one, a similar threshold can be reached, as we have demonstrated numerically.

Concluding this first section, we can say that the EM-BP algorithm of Ref. [7] seems to reach the same threshold  $\alpha_{BP}$ , either using a dense Gaussian matrix or a sparse binary one. However the use of a sparse matrix is computationally much faster than a dense one. Moreover, the use of binary elements, instead of Gaussian real values, allows for a better code optimization and eventually for hard-wiring encoding of the compression process.

#### IV. BLOCK-STRUCTURED SPARSE MATRICES

To overcome the secondary maximum of the free entropy, in Ref. [7] the authors use a kind of structured block matrix that helps to nucleate the correct solution. The idea is that the correct solution can be found for the first variables, and then it will propagate to all the signal. This idea is similar to the so-called spatial coupling, that is very useful for many different problems [16]. With this trick the authors of Ref. [7] reach a perfect recovery for almost any  $\alpha > \rho_0$  in the large  $N$  limit. Here we try to use a matrix with the same block structure, but sparsely filled. We divide the  $N$  variables into  $L$  groups of size  $N/L$  and the  $M$  measurements into  $L$  groups of size  $M_p = \alpha_p N/L$  in such a way that  $M = \sum_{p=1}^L M_p = \alpha N$  and  $1/L \sum_{p=1}^L \alpha_p = \alpha$ .

In this way the matrix  $\mathbf{F}$  is divided in  $L^2$  blocks, labeled with indices  $(p, q)$ . Each block is a sparse binary matrix with

$k$  elements different from zero for each row and  $h_p = \alpha_p k$  elements for each column, distributed according to Eq. (5), with  $J = J_{p,q}$ . As in Ref. [7] we choose  $J_{p,p-1} = J_1$ ,  $J_{p,p} = 1$ ,  $J_{p,p+1} = J_2$  and  $J_{p,q} = 0$  otherwise. The important ingredient to nucleate the correct solution is that in the first block  $\alpha_1 = (M_1/N)L > \alpha_{BP}$  holds. For simplicity we choose  $\alpha_1 = 1$  and  $\alpha_p = (L\alpha - 1)/(L - 1)$  for  $p \neq 1$ . The dependence of the recovery success from the parameters  $J_1$  and  $J_2$  is strong and the best results for  $\alpha = 0.5$  are obtained around  $J_1 = 4$  and  $J_2 = 1$ . We have chosen this two values for the following experiments also because we want to work with matrices whose elements are small integer values.

Similarly to the dense case, the use of a sparse structured matrix with blocks allows to overcome the dynamical transition at  $\alpha_{BP}$  and to nucleate the correct solution until  $\alpha$  very close to  $\rho_0$ . In Fig. 3 the mean critical threshold  $\rho_c(N)$  is shown for different signal lengths at a fixed compression rate  $\alpha = 0.5$ . On the  $x$  axis we have used the same scaling variable as in Fig. 5 and the best parameter  $a$  obtained from the fit of data in Fig. 5 also interpolates quite well data in Fig. 3. In the thermodynamic limit,  $\rho_c$  extrapolates to a value compatible with the optimal one,  $\alpha$ , and it is certainly much higher than the thresholds for the  $\ell_1$ -recovery and for EM-BP without any structure. We have done also a density evolution analysis, that confirms this result.

For each value of  $N$  and  $L$ , the mean critical threshold  $\rho_c$  is computed as follows. We randomly generate a block structured matrix  $\mathbf{F}$  with given  $N$  and  $L$ . We start with an original signal  $\mathbf{s}$  sufficiently sparse, which is recovered by the algorithm; then we add non-zero entries to the signal, and check whether the new signal can be recovered by the algorithm; we go on adding non-zero elements to the signal, until a failure in a perfect recovery occurs. The previous last value for  $\rho_0$  is the critical threshold for the matrix  $\mathbf{F}$ . The mean critical threshold is obtained by averaging over many different random matrices and signals, with the same values of  $N$  and  $L$ . The number of such random extractions goes from  $10^3$  for the largest  $N$  value up to  $10^4$  for the smallest  $N$  value.

The values of  $(N, L, k)$  used for the simulations shown in Fig. 3 are the following: (2250, 10, 9), (19000, 20, 19), (31200, 40, 39) and (49000, 50, 49). We need to increase both  $N$  and  $L$  if we want to obtain good results in the thermodynamic limit. However, if we change  $L$ , we must change  $k$  too. Indeed, in order to have the same number of elements per row and column for each of the  $L^2$  blocks, we must satisfy the conditions:  $(N/L)/M_p = k/h_p$  with  $k$  and  $h_p$  integer valued. We have used the smaller possible value for  $k$ , that is  $k = L - 1$ . The fact that it is impossible to keep  $k$  constant while increasing  $L$ , implies that these kind of block-structured matrices always become dense in the thermodynamic limit. This is a limitation of the block structure that we want to eliminate with the matrix proposed in the following Section.

#### V. AND WITHOUT BLOCKS?

The matrix proposed in Ref. [7] is not the only one that allows to reach the optimal threshold. In Ref. [17] the use of

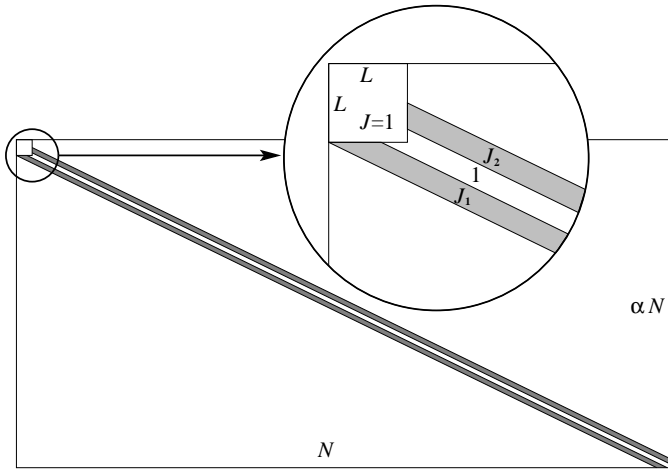


Fig. 4. Nearly one-dimensional sparse matrix with a first squared block of size  $L \times L$ , and non-zero elements in the stripes around the diagonal, can achieve compression and perfect recovery close to the theoretical bound in linear time.

other good dense, block-structured matrices is analyzed. However the block-structure is not so simple to handle if one wants to do analytical calculations in the continuum limit. Moreover in making these block-structured matrices sparse one has to be careful to find right values for  $L, M, N, M_p, \alpha_p, k$ . For these reasons we want to understand if the block structure is crucial, and, if not, we want to eliminate it.

We try a different structured sparse matrix (see Fig. 4), that we call striped matrix. It has one sparse square block of side  $L$  on the top left of the matrix with  $K = O(1)$  elements for each row and column extracted from (5) with  $J = 1$ . This is fundamental to nucleate the correct solution. Apart from this first block, the residual compression rate is  $\alpha' = \frac{M-L}{N-L}$ . Then we construct a one-dimensional structure, around the diagonal of the remaining matrix. For each column  $c > L$ , we put  $2K\alpha'$  non-zero elements, again extracted from (5), randomly placed in the interval of width  $2L\alpha'$  around the diagonal. One element with  $J = 1$  is always placed on the diagonal (actually on the position closest to the diagonal). For the remaining elements we use the following rules. If the element is at distance  $d \leq L\alpha'/3$  from the diagonal, we use  $J = 1$ . Otherwise, if its distance is  $d > L\alpha'/3$ , we use  $J = J_1$  below the diagonal and  $J = J_2$  above the diagonal. In this way the number of elements per column is constant, while the number of elements for row is a truncated Poisson random variable with mean  $2K$ : indeed there are no empty rows thanks to the rule of placing the first element of each column closest to the diagonal. When constructing the matrix we apply exactly the same rule to each column, but on the last  $L$  columns it may happen that a non-zero element has row index larger than  $M$ : these elements are then moved below the first squared matrix by changing row and column indices as follows:  $r \leftarrow r - (M - L)$  and  $c \leftarrow c - (N - L)$ .

In this way we have some kind of continuous one-dimensional version of the block-structured matrix discussed in the previous Section. Within this striped matrix ensemble

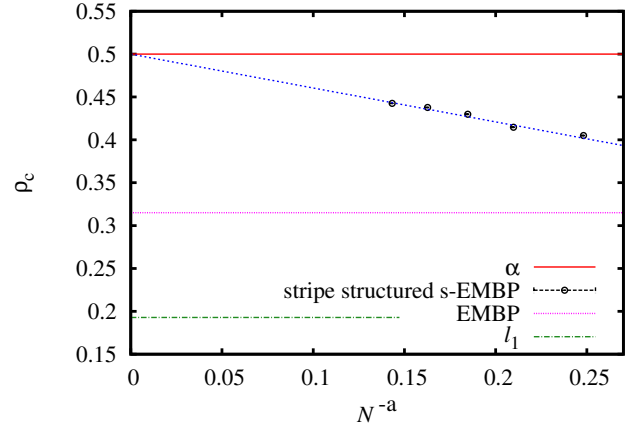


Fig. 5.  $\rho_c(N)$  with a sparse, striped matrix, as described in Section V for different sizes (from  $N = 2000$  to  $N = 40000$ ). The thresholds for the  $\ell_1$ -recovery and for EM-BP without structure are drawn for comparison. The best fitting parameter is  $a \simeq 0.18$  and leads to an extrapolation of  $\rho_c(N)$  in the thermodynamic limit compatible with  $\alpha$ .

the thermodynamic limit at fixed matrix sparsity can be taken without any problem, by sending  $N, L \rightarrow \infty$  at fixed  $L/N$  and fixed  $K = O(1)$ . In Fig. 5 we show the mean critical threshold reached by using striped matrices with a fixed ratio  $L/N = 1/50$  (the same used in the plot of Fig. 4) and different signal lengths. Perfect decoding up to  $\rho_c$  is again achieved by using the EM-BP algorithm. We have extrapolated the  $\rho_c(N)$  data to the thermodynamic limit by assuming the following behavior in the large  $N$  limit

$$\rho_c(N) = \rho_c(\infty) - bN^{-a} \quad (6)$$

Data in Fig. 5 have been plotted with the best fitting parameter  $a \simeq 0.18$  and the extrapolated value  $\rho_c(\infty)$  is perfectly compatible with the theoretical bound  $\alpha$ .

So we can conclude that the important ingredients to reach optimality is not the block structure, but the nearly one-dimensional structure, associated with an initial block with  $\alpha_1 > \alpha_{BP}$  to nucleate the correct solution.

It is worth noticing that the corresponding statistical mechanics model for these striped random matrices is a one-dimensional disordered model with an interaction range growing with the signal length as in a Kac construction. Models of this kind are analytically solvable, and show very interesting results [18].

The use of our striped sparse matrices allows for a great reduction in the computational complexity. Indeed, both times for measurement and recovery grow linearly with the size of the signal if sparse matrices are used, while they grow quadratically if dense matrices are used. In Fig. 6 the times for the measurement/recovery of a signal are shown for different signal lengths  $N$ . For this test, we used dense block-structured matrices and sparse striped matrices. The number of EM-BP iterations to reach the solution is roughly constant for different  $N$ . A quadratic fit for the dense case and a linear fit for the sparse one perfectly interpolate the data.

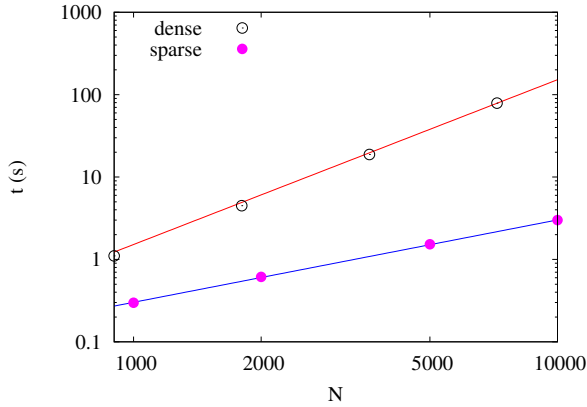


Fig. 6. Actual time (in seconds) for the recovery of a signal with dense and sparse matrices for different data length  $N$ . The data are fitted respectively by a quadratic and a linear function.

## VI. CONCLUSIONS AND FUTURE DEVELOPMENTS

We have introduced an ensemble of sparse random matrices  $F$  that, thanks to their particular structure (see Figure 4), allow to perform in a linear time the following operations:

- (i) measurement of a  $\rho_0$ -sparse vector  $s$  of length  $N$  by a linear transformation,  $y = Fs$ , in a vector  $y$  of length  $\alpha N$ ;
- (ii) perfect recovery of the original vector  $s$  by a message passing algorithm (Expectation Maximization Belief Propagation) for almost any parameter satisfying the theoretical bound  $\rho_0 < \alpha$ .

The main ingredients of these striped sparse matrices that allow to reach such good performances are the presence of a ‘seeding’ sparse square matrix in the upper left corner that nucleates a seed for the right solution and the one-dimensional structure along the diagonal that propagates such an initial seed to the complete right solution. Both the seeding and the one-dimensional structure have been already used in the past [7], [16], but in our new ensemble the matrices are sparse and this permits to perform all the operation in a time linear in the signal length.

We have also checked that sparse matrices perform as well as dense ones in case of block-structured matrices and for matrices with no structure at all.

Apart from the compressed sensing case, the sparsity of the matrix or equivalently the linear time complexity is essential in several applications [9]

In data streaming computing, one is typically interested in doing very quick measurements in constant time. For example, willing to measure the number of packets  $s_i$  with destination  $i$  passing through a network router, it is not possible to keep the vector  $s$  because is generally too long. Instead, a much shorter sketch of it,  $y = Fs$ , is measured, such that the very sparse vector  $s$  can be recovered from  $y$ . The sparsity of the matrix  $F$  is essential in order to be able to update the sketch  $y$  in constant time for each new packet passing through the router.

Another interesting application is the problem of group

testing, where a very sparse vector  $s \in \{0, 1\}^N$  is given and one is interested in performing the fewest linear measurements,  $y = Fs$ , that allow for the detection of the defective elements ( $s_i = 1$ ). In this case the sparsity of the matrix  $F$  is required by the experimental constraints: only if the tested compound  $y_\mu = \sum_i F_{\mu i} s_i$ , is made of very few elements of  $s$  the linear response holds and non-linear effects can be ignored.

However in the more general case, one does not observe directly the sparse signal  $s$  but rather a linear transformation of it,  $x = Ds$ , made with a dictionary matrix  $D$  (which is typically a Fourier or wavelet transformation, and thus is a dense matrix). In this more difficult case, one would like to design a sparse measurement matrix  $A$  such that the measurement/compression operation,  $y = Ax$ , is fast and the resulting observed data  $y$  is short thanks to the sparseness of  $s$ . The conflicting requirement is to have a fast recovery scheme, because now to recover the original signal one should solve  $\hat{s} = \operatorname{argmin} \|s\|_0$  subject to  $y = (AD)s$ , where  $AD$  is typically dense (e.g. in case of Fourier and wavelet transformations). So a very interesting future development of the present approach is to extend it to this more complex case.

## ACKNOWLEDGMENT

FR-T acknowledges useful discussions with F. Krzakala, M. Mézard and L. Zdeborova, and financial support by the Italian Research Minister through the FIRB Project No. RBFR086NN1 on “Inference and Optimization in Complex Systems: From the Thermodynamics of Spin Glasses to Message Passing Algorithms”.

YK acknowledges support by grants from the JSPS (KAK-ENHI No. 22300003) and the Mitsubishi foundation.

## REFERENCES

- [1] E. J. Candès and M. B. Wakin, “An Introduction To Compressive Sampling,” *IEEE Signal Processing Magazine*, vol. 25, pp. 21–30, 2008.
- [2] M. A. T. Figueiredo, R. D. Nowak and S. J. Wright, “Gradient Projection for Sparse Reconstruction: Application to Compressed Sensing and Other Inverse Problems,” *IEEE Journal of Selected Topics in Signal Processing* vol. 1, pp. 586–597, 2007.
- [3] R. Cartrand and W. Yin, “Iteratively reweighted algorithms for compressive sensing,” in *IEEE International Conference on Acoustics, Speech and Signal Processing, 2008*, pp. 3869–3872, 2008.
- [4] W. Yin, S. Osher, D. Goldfarb and J. Darbon, “Bregman Iterative Algorithms for  $\ell_1$ -Minimization with Applications to Compressed Sensing,” *SIAM J. Imaging Sciences*, vol. 1, pp. 143–168, 2008.
- [5] T. Blumensath and M. E. Davies, “Iterative hard thresholding for compressed sensing,” *Applied and Computational Harmonic Analysis*, vol. 27, pp. 265–274, 2009.
- [6] D. L. Donoho, A. Maleki and A. Montanari, “Message-passing algorithms for compressed sensing,” *PNAS*, vol. 106, 18914–18919, 2009.
- [7] F. Krzakala, M. Mézard, F. Sausset, Y. F. Sun and L. Zdeborova, “Statistical-physics-based reconstruction in compressed sensing,” *Phys. Rev. X*, vol. 2, 021005 (18pages), 2012.
- [8] R. Berinde and P. Indyk, “Sparse recovery using sparse random matrices,” Preprint, 2008.
- [9] A. Gilbert and P. Indyk, “Sparse Recovery Using Sparse Matrices,” *Proceedings of the IEEE*, vol. 98, pp. 937–947, 2010.
- [10] M. Akçakaya, J. Park and V. Tarokh, “A Coding Theory Approach to Noisy Compressive Sensing Using Low Density Frames,” *IEEE Trans. on Signal Processing*, vol. 59, pp. 5369–5379, 2011.
- [11] Y. Kabashima and T. Wadayama, “A signal recovery algorithm for sparse matrix based compressed sensing,” arXiv:1102.3220, 2011.

- [12] D. Baron, S. Sarvotham and R. G. Baranuik, "Bayesian Compressive Sensing via Belief Propagation," *IEEE Trans. on Signal Processing*, vol. 58, pp. 269–280, 2010.
- [13] S.-Y. Chung, G. D. Forney Jr., T. J. Richardson and R. Urbanke, "On the Design of Low-Density Parity-Check Codes within 0.0045 dB of the Shannon Limit," *IEEE Comm. Lett.*, vol. 58 no.2, pp. 58-60, 2000.
- [14] S. Rangan, "Estimation with random linear mixing, belief propagation and compressed sensing," *Proc. Conf. Inf. Sci. Syst.*, Princeton, NJ, pp. 1–6, 2010.
- [15] D. J. Thouless, P. W. Anderson and R. G. Palmer, "Solution of 'Solvable model of a spin glass'," *Phil. Mag.*, vol. 35, pp. 593–601, 1977.
- [16] S. H. Hassani, N. Macris and R. Urbanke, "Coupled graphical models and their thresholds," arXiv:1105.0785, 2011.
- [17] F. Krzakala, M. Mézard, F. Sausset, Y. Sun and L. Zdeborova, "Probabilistic Reconstruction in Compressed Sensing: Algorithms, Phase Diagrams, and Threshold Achieving Matrices," arXiv:1206.3953, 2012.
- [18] S. Franz and A. Montanari, "Analytic determination of dynamical and mosaic length scales in a Kac glass model," *J. Phys. A*, vol. 40, pp. F251–F257, 2007.